IEEE Access
Multidisciplinary ⋮ Rapid Review ⋮ Open Access Journal

Received 17 March 2023, accepted 3 April 2023, date of publication 12 April 2023, date of current version 10 May 2023.
Digital Object Identifier 10.1109/ACCESS.2023.3266443

RESEARCH ARTICLE

A Four-Sided Matching Game for Energy-Efficient Scheduling in Narrowband-IoT Networks

FARAH YASSINE[1,2], **MELHEM EL HELOU**[1], (Senior Member, IEEE), **SAMER LAHOUD**[1,3], AND **OUSSAMA BAZZI**[2]
[1]Ecole Supérieure d'Ingénieurs de Beyrouth, Saint Joseph University of Beirut, Mansourieh, Lebanon
[2]Ecole Doctorale des Sciences et Technologies, Lebanese University, Hadath, Beirut, Lebanon
[3]IRISA Laboratory, University of Rennes, 35000 Rennes, France

Corresponding author: Farah Yassine (farah.yassine1@net.usj.edu.lb)

ABSTRACT This paper studies the uplink resource allocation problem in NB-IoT networks. We aim to maximize the network's energy efficiency to serve devices in need for long battery lifetime. Also, the network energy efficiency is affected by the associated UEs to candidates, carrying the scheduling information for UEs. For this reason, we investigate the joint resource allocation and Candidate-UE association problem in the uplink (UL) in NB-IoT. The resource allocation problem allocates the UEs with the suitable scheduling delay value and subcarrier indication field. The Candidate-UE association problem selects the appropriate UE for each candidate. The optimization variables involved in the joint problem are divided into binary association variables and binary resource allocation variables. This makes it hard to solve the joint problem since its optimization variables are of combinatorial nature. To this end, we formulate the joint problem as a four-sided matching game that ranks the UEs, candidates, the scheduling delay values and subcarrier indication fields while considering maximizing the energy efficiency as a preference metric. We then describe a four-sided matching game algorithm to solve the problem. The simulation results highlight the proposed algorithm's effectiveness compared to other algorithms in the obtained network energy efficiency.

INDEX TERMS Energy efficiency, matching theory, NB-IoT, resource allocation.

I. INTRODUCTION

Narrowband-Internet of Things (NB-IoT) technology is one of the low power wide-area (LPWA) technologies, designed by the third-generation partnership project (3GPP), to meet the requirements of the massive machine-type communications (mMTC) [1]. The main purpose of designing NB-IoT is to serve massive number of connections with high reliability over narrow bandwidth [2]. By 2027, NB-IoT, in addition to LTE-M, are expected to enable the communication of approximately 51 percent of all cellular IoT connections [3]. Accordingly, efficient utilization of the radio resources in NB-IoT networks is important to achieve massive number of connections, with satisfying quality of service.

NB-IoT supports the allocation of resource unit (RU), a basic radio resource allocation unit carrying the transmitted data, through which devices are allocated subcarriers instead of the whole resource block. This enables allocating devices small amount of the bandwidth, thus freeing portions of the bandwidth for other devices, ending up with multiple concurrent connections. Also, RU allocation serves in ensuring reliable transmissions by allocating devices small portion of the bandwidth [4]. This concentrates the transmission energy on the small bandwidth ending up with strengthened signals.

With the support of RU allocation, existing scheduling procedures are not suitable for NB-IoT networks. The LTE scheduling procedure allocates the devices the entire physical resource block, while in NB-IoT the allocation is more granular and performed at the level of subcarriers (SC). Also, NB-IoT aims to serve devices that need long battery life [4]. As energy efficiency is a key issue in NB-IoT scheduling, NB-IoT networks need energy-efficient scheduling schemes considering NB-IoT unique specification of RU.

The scheduling in NB-IoT can be divided into two procedures: link adaptation and resource allocation. The correlation between the two procedures is investigated in our

The associate editor coordinating the review of this manuscript and approving it for publication was Abdel-Hamid Soliman.

previous work [5]. The link adaptation procedure is performed at the level of each device independently based on the device's radio conditions. However, in the resource allocation procedure, the resources are divided among the devices based on the allocated scheduling parameters. The scheduling parameters involved in the resource allocation procedure are the subcarrier indication field determining the RU type and subcarrier set, in addition to the scheduling delay value. The scheduling parameters are explained in detail in Section III.

NB-IoT scheduling occurs every narrowband physical downlink control channel (NPDCCH) Period (NP), and the scheduling information for each device is carried by a downlink control indicator (DCI). A DCI carries the scheduling information for only one device so that device can determine its associated uplink resources for its uplink data transmission. However, the transmission of a DCI, carrying the scheduling information for a device, is repeated to reduce the transmission errors [6]. The downlink subframes carrying one DCI are known as candidates such that each candidate is associated to only one device. As the number of candidates in each NPDCCH Period (NP) is finite, the selection of a device associated to a candidate impacts the network energy efficiency and the overall performance.

In this context, we aim to study the joint problem of NB-IoT resource allocation procedure and the process of associating devices (UE) to candidates (Candidate-UE association) in the uplink with the objective of maximizing the network energy efficiency. The optimization variables consider the binary association variables and the binary resource allocation variables. Due to the combinatorial nature of the optimization variables, it is hard to get the optimal solution of the joint problem for real-sized networks.

As the process of selecting for each candidate the best UE is affected by the association and the resource allocation parameters (scheduling delay value and subcarrier indication field) to other UEs, this paper considers the matching theory to model and investigate the mutual interactions among the players in NB-IoT networks [7]. We formulate the joint problem as a many-to-many multivariate matching game. The optimization variables consider the binary association variables including the UEs and the candidates, and the binary resource allocation variables including the scheduling delay value and subcarrier indication field. Then, we define a preference metric to match these variables with each other. Accordingly, we model the problem as a four-sided matching game. Then, we propose an algorithm to solve the problem. The main contributions of the paper are described as follows:

- To the best of our knowledge, this is the first paper that investigates the resource allocation problem and the Candidate-UE association problem as one joint problem in the uplink in NB-IoT networks using matching game theory.
- We believe that this paper is the first to formulate a four-sided matching game in NB-IoT networks involving UEs, candidates, scheduling delay values, and subcarrier indication fields to model the joint resource allocation and Candidate-UE association optimization problem, with an objective of maximizing the network energy efficiency.
- The simulation results focus on investigating the impact of the proposed four-sided matching game algorithm on the NB-IoT performance in terms of the achieved sum-energy efficiency, while comparing it with well-known heuristic methods.

The remainder of the paper is structured as follows. Section II presents the related work. Section III describes the system model including the scheduling parameters and constraints. Section IV formulates the joint optimization problem. Section V models the joint problem as a four-sided matching game and develops a four-sided many-to-many matching algorithm. Section VI interprets the simulation results. Section VII presents a detailed discussion of the obtained simulation results. Finally, Section VIII sums up the conclusion.

II. RELATED WORKS

Scheduling problem is investigated in different IoT networks as in [8] and [9]. The authors in [8] investigate the scheduling problem for managing the generated tasks of Industrial Internet of Things (IIoT) applications in fog environments while satisfying energy and delay constraints. The authors, in [9], investigate the joint optimization problem of beamforming, power control, and energy in SWIPT-Enabled IoT Networks. Their investigation aims to enhance the performance of the communication between the base stations or access points to the served mobile nodes using deep reinforcement learning and non-cooperative game theory model. As for NB-IoT network, many recent articles study various aspects of the scheduling problem as in [10] and [11]. The authors in [10] consider the power-saving mode while studying the NB-IoT scheduling problem to save more energy while achieving massive connection. The authors in [11] investigate the NPDCCH offset mechanism in resource allocation problem in NB-IoT with the objective of minimizing the consumed radio resources.

The NB-IoT link adaptation problem is investigated in [12], [13], [14], [15], [16], [17], [18], and [19]. In [12], an efficient link adaptation method is proposed for NB-IoT networks. The proposed method selects the appropriate modulation and coding scheme (MCS) and number of repetitions reducing the number of narrowband uplink shared channel (NPUSCH) and NPDCCH transmissions. A dynamic link adaptation strategy, selecting the MCS level and repetition number, is proposed in [13] for NB-IoT uplink transmissions. In [14], the authors propose a link adaptation strategy based on a look-up table to select appropriate number of repetitions and MCS level. The authors, in [15], propose a 2D link adaptation method. The method searches for the optimal number of repetitions and MCS level that improve the spectral efficiency and reduce the consumed power. Neither [12],

[13], [14], or [15] considered the allocation of the RU type, as a unique specification in NB-IoT, in their proposed link adaptation schemes. The authors in [16] and [17] propose link adaptation schemes considering the RU type allocation in addition to the MCS level and number of repetitions determinations. The authors in [16] use derived analytical expressions to study the impact of the RU type, repetitions, and MCS. Also, the authors propose a link adaptation scheme that aims to minimize the transmission time. The authors in [17] design hybrid link adaptation scheme that aims to achieve reliability, optimal uplink latency, and coverage. However, their work considers ideal channel estimation for simplicity. Our previous work [18] and [19] study the NB-IoT link adaptation problem. In [18], we study the impact of each of the type of RU, number of repetitions, and MCS level on the link adaptation performance in NB-IoT. Our work in [19] presents an extension to [18]. In [19], we provide a link-level investigation where we study the impact of the received power and the data size on the NB-IoT performance.

The resource allocation in NB-IoT is the main concern of many recent studies as in [20], [21], [22], and [23]. In [20], an iterative resource allocation algorithm is proposed for multi-cell cellular NB-IoT networks. The proposed algorithm aims to enhance the resource allocation through managing the inter-cell interference while maximizing the network rate. However, their allocation is performed at the level of the entire resource block as in LTE without considering the RU type allocation. The authors in [21] propose an uplink resource allocation algorithm for NB-IoT. The proposed algorithm allocates the devices the appropriate RU type minimizing the consumed subframes, but the same RU type is allocated for all the devices in a scheduling period. The authors in [22] propose an energy efficient scheduling algorithm for NB-IoT networks. The proposed algorithm minimizes the consumed energy per device while improving spectrum utilization. Nevertheless, the scheduling delay between the uplink and downlink transmissions is not considered. In [23], a suboptimal algorithm is proposed for the resource allocation problem in NB-IoT. The proposed algorithm aims to maximize the data rate, through selecting the best RU type giving the highest data rate while fitting in the remaining resources. However, the algorithm considers only the RU type while neglecting the remaining scheduling parameters. This article, compared to [20], [21], [22], and [23], considers the complete parameters set of RU type, MCS, repetition number, resource assignment, scheduling delay, and the subcarrier set involved in NB-IoT scheduling, inaddition to the main NB-IoT devices' requirements of reliable transmission, delay, and resource allocation constraints summarized in Table 1. "-" in Table 1 means not mentioned.

The matching theory is applied in different wireless networks due to its stability and optimality properties [24], while managing resource allocation and user association problems with different objectives as in [25], [26], and [27]. In [25], the matching game is utilized to study the joint user association and resource allocation problems in orthogonal frequency-division multiple-access networks (OFDMA) considering full-duplex (FD). The authors in [26] consider the matching game to model the joint resource allocation problem and user association problem in heterogeneous cellular networks (HCNs) considering full-duplex mode. In [27], the authors apply matching game to optimize the selection of the devices for NB-IoT networks in the uplink. The authors propose a non-orthogonal multiple access (NOMA) scheme-based matching game to maximize the network rate and improve the capacity. However, none of the work considers the matching game to model and study the joint user association and resource allocation problem in NB-IoT networks.

TABLE 1. Supported scheduling parameters and constraints.

Parameters and constraints	[20]	[21]	[22]	[23]	This work
RU type	NO	NO	YES	YES	YES
MCS	YES	YES	YES	-	YES
Repetitions number	YES	YES	YES	-	YES
Resource assignment	YES	YES	YES	-	YES
Scheduling delay	YES	YES	NO	-	YES
Subcarrier set	YES	YES	-	-	YES
Reliable transmission	YES	YES	YES	YES	YES
Delay	NO	NO	YES	NO	YES
Resource allocation	NO	YES	-	YES	YES

III. SYSTEM MODEL

A NB-IoT network is considered consisting of a base station (BS) and I devices. We define the set of devices as $\mathfrak{I} = \{1, 2, 3, .., I\}$. A device i, where $i \in \{1, .., I\}$, transmits to the BS an uplink data of size denoted by D_i (bits) at a transmission power p_{t_i} such that $p_t^{min} \leq p_{t_i} \leq p_t^{max}$. p_t^{min} and p_t^{max} denote respectively the minimum and the maximum transmission powers. Each device must upload its data before its delay deadline d_i (ms), to ensure quality of service (QoS).

A device transmits its uplink data using the resources defined by the scheduling information. The scheduling information for a device is carried by one downlink control information (DCI). A device monitors successive narrowband physical downlink control channel (NPDCCH) subframes, known as search spaces, to decode its corresponding DCI carried by a NPDCCH subframe. The length of the NPDCCH search space represents the number of NPDCCH subframes, determined by a system parameter R_{max}. The NB-IoT uplink scheduling occurs every NPDCCH Period (NP). NP is the time interval between two successive NPDCCH opportunities. R_{max} and G, a system parameter [6], [28], determine the NP length, where NP length equals $R_{max} \cdot G$. The number of narrowband uplink shared channel (NPUSCH) is equal to the NP length. The values of R_{max} and G can be adapted to get different NP lengths. This is known as NPDCCH period adaptation problem investigated in [29].

In general, the scheduling information for each device is carried by only one DCI. However, a DCI, corresponding to one device, is retransmitted r_{DCI} times to decrease the transmission errors [6]. The NPDCCH subframes transmitting one

TABLE 2. The main scheduling fields.

Scheduling Field	Value
Subcarrier Indication Field (I^{sc})	$0 \sim 63$
Repetition Number Field (I^{rep})	$0 \sim 7$
Resource Assignment Field (I^{RU})	$0 \sim 7$
Modulation and Coding Scheme Field (I^{MCS})	$0 \sim 13$
Scheduling Delay Field (I^{delay})	$0 \sim 3$

DCI are known as candidates as clarified in Fig. 1. J denotes the number of candidates in an NP, where $J = R_{max}/r_{DCI}$. We define the set of candidates in an NP as $\mathfrak{J} = \{1, 2, 3, .., J\}$. We define a binary association variable $\eta_{i,j}$ to indicate if a device i is associated to a candidate j as expressed in (1).

$$\eta_{i,j} = \begin{cases} 1, & \text{if device } i \text{ is associated to candidate } j \\ 0, & \text{otherwise} \end{cases} \tag{1}$$

A DCI carries the scheduling information results, specified by the BS, for a device. The BS needs to allocate for each device i, the optimal combination of the scheduling parameters while guaranteeing reliable transmission, meeting the delay requirements, and satisfying the allocation constraints.

A. NB-IoT UPLINK SCHEDULING PARAMETERS

Table 2 summarizes the main scheduling parameters fields, and their corresponding values, carried by a DCI for uplink transmission [6].

1) SUBCARRIER INDICATION FIELD (I^{sc})

The RU is the smallest unit that maps a transport block in the uplink. Multiple types of RUs are supported in NB-IoT depending on the subcarrier spacing. For a subcarrier spacing of 15 kHz, both single-tone and multi-tone transmissions are supported. Single-tone transmission includes the RU type 1 tone, while multi-tone transmission includes the RU types 3, 6, and 12 tones. Subcarrier spacing 3.75 kHz only supports single-tone transmission. In this paper, we consider the standard subcarrier spacing 15 kHz. Accordingly, each device can be allocated one of the RU types (y): 1-tone, 3-tone, 6-tone, and 12-tone. We define an integer variable q to identify the RU type as described in (2).

$$q = \begin{cases} 1, & y = 12 \quad \text{tones} \\ 2, & y = 6 \quad \text{tones} \\ 3, & y = 3 \quad \text{tones} \\ 4, & y = 1 \quad \text{tone} \end{cases} \tag{2}$$

Only one RU type can be allocated to a device i to transmit its uplink data in an NP p. The RU type is allocated based on the radio conditions of the device and the scheduling objective. We define a binary variable $v_{p,i,q} \in \{0, 1\}$ indicating if RU type q is allocated to device i as in (3).

$$\sum_{q=1}^{4} v_{p,i,q} \leq 1, \forall p \in P, \forall i \in \mathfrak{T} \tag{3}$$

TABLE 3. Characteristics of the different RU types for subcarrier spacing = 15 kHz.

Number of tones (RU Type)	Number of timeslots	RU duration time (ms)	RU bandwidth (kHz)	Transmission format
1-tone	16	8	15	Single-Tone
3-tone	8	4	45	Multi-Tone
6-tone	4	2	90	Multi-Tone
12-tone	2	1	180	Multi-Tone

TABLE 4. Subcarrier indication field values and its corresponding RU type and subcarrier sets.

Subcarrier Indication Value (I_l^{sc})	RU Type	Subcarrier Set
$0 \sim 11$	1 tone	I_l^{sc}
12∼15	3 tones	$3 \cdot (I_l^{sc} - 12) + \{0, 1, 2\}$
16∼17	6 tones	$6 \cdot (I_l^{sc} - 16) + \{0, 1, 2, 3, 4, 5\}$
18	12 tones	$\{0, 1, 2, 3, ..., 11\}$
19∼63	Reserved	

The RU type defines the duration and the number of subcarriers occupied by a RU denoted by t and β respectively as shown in (4) and (5).

$$\beta_{p,i} = 12 \cdot v_{p,i,1} + 6 \cdot v_{p,i,2} + 3 \cdot v_{p,i,3} + 1 \cdot v_{p,i,4} \tag{4}$$

$$t_{p,i} = 1 \cdot v_{p,i,1} + 2 \cdot v_{p,i,2} + 4 \cdot v_{p,i,3} + 8 \cdot v_{p,i,4} \tag{5}$$

The supported RU types for subcarrier spacing of 15 kHz with their corresponding timeslots and number of subcarriers are summarized in Table 3.

Equations (4) and (5) ensure that the total allocated number of subcarriers and the total duration, spanned by a RU for a device i, satisfy the RU characteristics described in Table 3. This is achieved through $v_{p,i,q}$ which is equal to one for only one q as guaranteed in (3).

We define the set of values of the subcarrier indication field as $\mathfrak{L} = \{1, 2, 3, .., L\}$. The value of the subcarrier indication field I_l^{sc}, where $l \in \mathfrak{L}$, determines the RU type q and the subcarriers set n^{sc} as described in Table 4. For instance, for I_1^{sc}, the RU type is 1-tone, and the RU occupies subcarrier set $n_1^{sc} = \{0\}$.

The relation between the value of the subcarrier indication field with the RU type and the subcarrier sets allocated for a device i in NP p is shown in (6) and (7).

$$I_{p,i,l}^{sc} = I_l^{sc1} \cdot v_{p,i,1} + I_l^{sc2} \cdot v_{p,i,2} + I_l^{sc3} \cdot v_{p,i,3} + I_l^{sc4} \cdot v_{p,i,4}, \tag{6}$$

where $I_l^{sc1} = 18$, $I_l^{sc2} \in \{16, 17\}$, $I_l^{sc3} \in \{12, 13, 14, 15\}$, and $I_l^{sc4} \in \{0, 1, .., 11\}$.

$$\begin{aligned} n_{p,i,l}^{sc} = &\{0, 1, 2, 3, 4, 5, 6, 7, 8, 9, 10, 11\} \cdot v_{p,i,1} \\ &+ (6 \cdot (I_{p,i,l}^{sc2} - 16) + \{0, 1, 2, 3, 4, 5\}) \cdot v_{p,i,2} \\ &+ (3 \cdot (I_{p,i,l}^{sc3} - 12) + \{0, 1, 2\}) \cdot v_{p,i,3} \\ &+ I_{p,i,l}^{sc4} \cdot v_{p,i,4} \end{aligned} \tag{7}$$

2) REPETITION NUMBER FIELD (I^{rep})

NB-IoT serves devices in challenging radio conditions through exploiting repetitions. The transmissions in NB-IoT

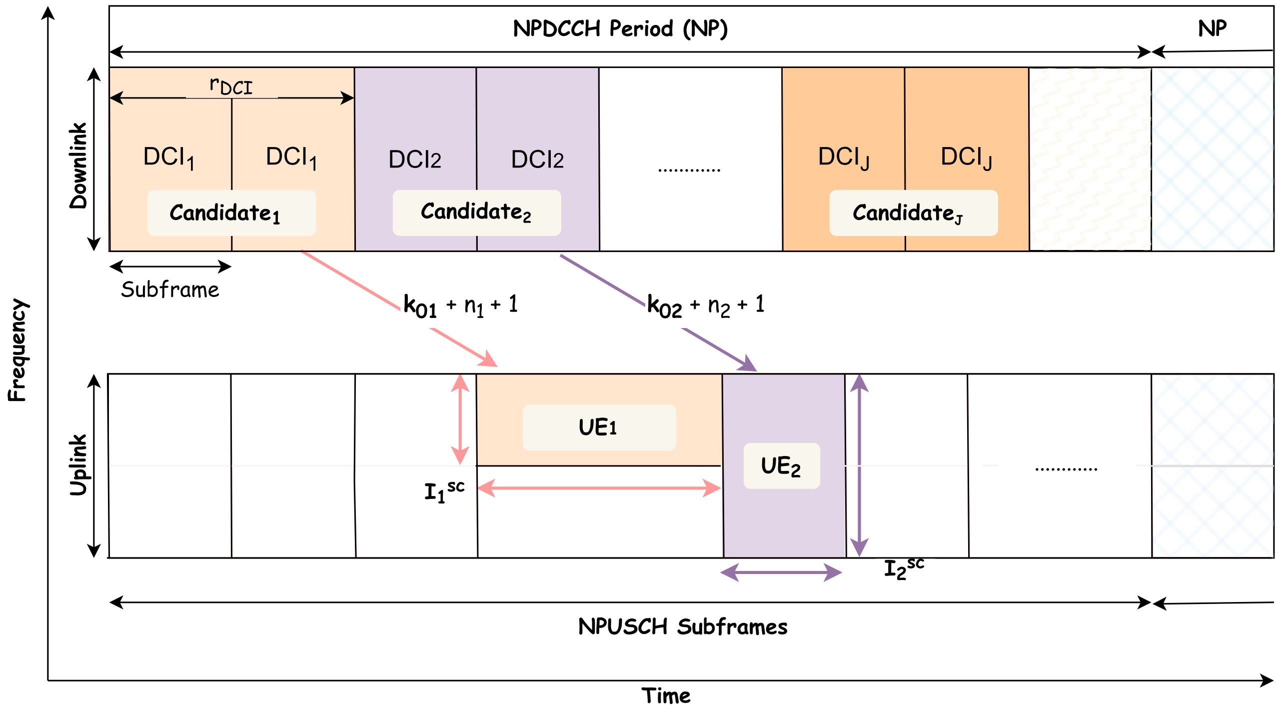

FIGURE 1. A simplified illustration of the NB-IoT scheduling.

are repeated to ensure reliable transmissions through decreasing the threshold signal-to-noise ratio. NB-IoT blindly repeats the RU transmission. Table 5 shows the I^{rep} values and their corresponding number of repetitions r allocated for the uplink transmissions.

TABLE 5. The supported uplink number of repetitions in NB-IoT.

Repetition Number Field (I^{rep})	0	1	2	3	4	5	6	7
Repetition Number Value (r)	1	2	4	8	16	32	64	128

3) RESOURCE ASSIGNMENT FIELD (I^{RU})

I^{RU} specifies the number of continuous RUs (u) allocated to a device without considering the repetition. Table 6 shows the different values of I^{RU} with their corresponding u. The allocated number of repetitions is multiplied with the associated resource assignments value to get the total number of RUs allocated to a device for its complete transmission.

TABLE 6. The supported uplink resource assignment in NB-IoT.

Resource Assignment Field (I^{RU})	0	1	2	3	4	5	6	7
Resource Assignment Value (u)	1	2	3	4	5	6	8	10

4) MODULATION AND CODING SCHEME FIELD (I^{MCS})

I^{MCS} indicates the value of the modulation and coding scheme level denoted by m. In NB-IoT, there are 11 different MCS levels $\{0, 1, 2, .., 10\}$ and 14 different MCS levels $\{0, 1, 2, .., 13\}$ for single-tone and multi-tone transmissions, respectively. The MCS level and the resource assignments determine the transport block size (TBS). The allocation of the MCS level is dependent on device's radio conditions. Devices with bad radio conditions are allocated low MCS levels. However, devices with good channel qualities are allocated higher MCS levels to improve the network data rate.

5) SCHEDULING DELAY FIELD (I^{delay})

We define the set of scheduling delay values as $\mathfrak{K} = \{1, 2, 3, .., K\}$. I^{delay} determines the scheduling delay value k_{0_k} where $k \in \mathfrak{K}$. k_{0_k} specifies the time separating the last DCI of a device and its allocated start uplink subframe. During this time, the device decodes the DCI message and switches from reception to transmission mode. Table 7 shows the different values of the scheduling delay.

TABLE 7. The scheduling delay values supported for the uplink scheduling.

Scheduling Delay Field (I^{delay})	0	1	2	3
Scheduling Delay Value (k_{0_k}) in ms	8	16	32	64

The allocated k_{0_k} and the last NPDCCH subframe, denoted by ($n_{p,i}$), carrying its DCI determine the allocated start NPUSCH subframe ($sb_{p,i}$) of a device i in NP p according to (8), as shown in Fig. 1.

$$sb_{p,i} = k_{0_{i,k}} + n_{p,i} + 1 \tag{8}$$

B. SCHEDULING OBJECTIVE

Our goal is to maximize energy efficiency, as NB-IoT devices need long battery life. We define energy efficiency as the ratio of data rate over the consumed energy as expressed in (9). The data rate (DR) is the ratio of the data size over the transmission duration as shown in (10). The consumed energy (CE) is expressed in (11) as the transmission duration multiplied with the transmitted power.

$$EE(r,u,m,q) = \frac{DR(r,u,m,q)}{CE(r,u,m,q)} = \frac{D}{p_t \cdot (u \cdot t \cdot r)^2} \tag{9}$$

$$DR(r,u,m,q) = \frac{D}{u \cdot t \cdot r} \tag{10}$$

$$CE(r,u,m,q) = p_t \cdot u \cdot t \cdot r \tag{11}$$

We define the transmission duration as the resource assignment u multiplied with the duration of the RU t and the number of repetition r.

C. SCHEDULING CONSTRAINTS

NB-IoT scheduling needs to ensure reliable transmission and satisfy delay constraint and the resource allocation constraint, to meet feasible uplink scheduling.

1) RELIABLE TRANSMISSION CONSTRAINT

A transmission is considered reliable if the received signal-to-noise ratio (SNR), denoted by S_{rx}, is greater than or equal to the required signal-to-noise ratio, denoted by S_{req}, for successful decoding of the received signal as expressed in (12).

$$S_{rx} \geq S_{req} \tag{12}$$

Equation (13) expresses the received SNR. G_t, G_r, L_{shadow}, L_{path}, $L_{penetration}$, w, N_0, f, and γ denote the transmitter antenna gain, the receiver antenna gain, the shadow fading effect, the path loss, the penetration loss, bandwidth of the RU, the receiver noise spectral density, interference level, and the indoor/outdoor binary indicator, respectively.

$$S_{rx}(q) = \frac{p_t \cdot G_r \cdot G_t}{L_{path} \cdot L_{shadow} \cdot \gamma L_{penetration} \cdot (w \cdot N_0 + f)} \tag{13}$$

We consider the cross-subframe channel estimation [30] to estimate the S_{req} as expressed in (14). Realistic channel estimations limit the coverage extension, due to a channel estimation error σ. Cross-subframe technique reduces these limitations, through averaging the channel estimates over multiple consecutive subframes. The estimation of S_{req} is expressed as follows:

$$(2^{\frac{R_b}{w \cdot B_{eff}}} - 1).S_{eff} = \frac{r.(\sigma + S_{req})}{(\sigma + 1 + \frac{\sigma}{S_{req}})(1 + \frac{\sigma}{2.S_{req}})}. \tag{14}$$

R_b, w, B_{eff} and S_{eff} denote the transmission data rate measured in bits/s, the bandwidth of the RU, the bandwidth efficiency and SNR efficiency of NB-IoT technology, respectively. B_{eff} and S_{eff} are obtained using curve fitting in the 3GPP link-level simulation results [31], [32].

Equation (15) expresses the linear dependency of the estimation error σ and S_{req}. c_1 and c_2 are constants obtained using the link-level simulations [31], [32].

$$\sigma_{dB} = c_1 \cdot S_{req,dB} + c_2 \tag{15}$$

The theoretical transmission data rate (R_b) is expressed as:

$$R_b(u,t,m) = \frac{B + C}{u \cdot t}, \tag{16}$$

where C, B, t and u denote the cyclic redundancy check code size (bits), transport block size (bits), the durations of the RU, and the resource assignment, respectively.

The maximum TBS, denoted by B_{max}, is dependent from the selected MCS m and the resource assignment u. The 3GPP Release 14 standard [6] defines the size of B_{max} at the MAC layer ranging from 2 bytes to 217 bytes and 317 bytes for single-tone and multi-tone transmissions, respectively. The size of B is affected by the application payload and higher-layer protocol overhead. The size of B must be lower than or equal to B_{max} as

$$B \leq B_{max}(u, m) \tag{17}$$

2) DELAY CONSTRAINT

A device needs to transmit its data to the BS before its delay deadline d_i. Equation (18) expresses the delay constraint as:

$$sb(k_{0_k}) + u \cdot r \cdot t \leq d \tag{18}$$

where $u \cdot r \cdot t$ denotes the transmission duration in the uplink.

In this paper, we consider sb feasible if it is within the current NP as shown in (19).

$$1 \leq sb \leq N, \tag{19}$$

where the length of the NP is denoted by N such that $N = R_{max} \cdot G$.

The device needs to upload all its uplink data within the current NP as expressed in (20).

$$sb + u \cdot r \cdot t - 1 \leq N \tag{20}$$

3) RESOURCE ALLOCATION CONSTRAINT

To avoid overlapping devices, a resource element is allocated for only one device. Accordingly, a binary allocation variable $x_{p,s,c,i} \in \{0, 1\}$ is defined indicating if subcarrier c at subframe s is allocated to a device i in NP p or not as expressed in (21).

$$\sum_{i=1}^{I} x_{p,s,c,i} \leq 1, \quad \forall p, \forall s, \forall c \tag{21}$$

Equation (22) ensures that a number of $u \cdot r \cdot t$ uplink subframes are assigned to device i in NP p.

$$\sum_{s=1}^{N} x_{p,s,c,i} = u_i \cdot r_i \cdot t_i, \quad \forall p, \forall i, \forall c \tag{22}$$

Equation (23) ensures the contiguity of the allocated uplink subframes for device i.

$$\sum_{s=1}^{N} |(x_{p,s,c,i} - x_{p,s+1,c,i})| \leq 2, \quad \forall p, \ \forall i, \ \forall c \tag{23}$$

Equation (24) ensures that each allocated subframe occupies number of subcarriers denoted by β of the allocated $n^{sc}_{p,i,l}$.

$$\sum_{s=1}^{N} \sum_{c_1}^{c_{end}} x_{p,s,c,i} = \beta_i \cdot (u_i \cdot r_i \cdot t_i), \quad \forall p, \ \forall i, \tag{24}$$

where $c_1 = \min n^{sc}_{p,i,l}$ and $c_{end} = \max n^{sc}_{p,i,l}$.

4) ASSOCIATION CONSTRAINT

Equations (25) and (26) define the association constraints. Equation (25) ensures that each device i can be associated to only one candidate j.

$$\sum_{j=1}^{J} \eta_{i,j} \leq 1, \quad \forall i \in \mathfrak{I} \tag{25}$$

Equation (26) ensures that each candidate j carries the scheduling information for only one device i.

$$\sum_{i=1}^{I} \eta_{i,j} \leq 1, \quad \forall j \in \mathfrak{J} \tag{26}$$

IV. PROBLEM FORMULATION

In the NB-IoT scheduling, the BS must select the optimal combination of the scheduling parameters of number of repetitions r, resource assignments u, MCS level m, scheduling delay k_0, the RU type q and the subcarrier set n_{sc}. The optimal combination is the one maximizing energy efficiency, while ensuring reliable transmission, satisfying delay requirements, and respecting the allocation constraint.

The scheduling problem can be divided into link adaptation problem and resource allocation problem. The link adaptation problem aims to maximize the energy efficiency per device while selecting the best feasible combination of MCS level m_i, number of repetitions r_i, RU type q_i, and the resource assignment u_i. The combination is considered feasible if it guarantees reliable transmission and satisfying delay constraints. In our previous work [5], we formulated the general link adaptation problem applied for each device i as follows:

$$\begin{aligned} &\max_{r,u,m,q} \ EE(r, u, m, q) \\ &s.t \ S_{rx}(q) \geq S_{req}(m, u, r) \\ &\quad p_t^{min} \leq p_t \leq p_t^{max} \\ &\quad r \cdot t \cdot u \leq d \\ &\quad B \leq \max B(u, m) \end{aligned} \tag{27}$$

In this work, we utilize the link adaptation algorithm proposed in our previous work in [18] to collect all the feasible link adaptation combinations of MCS m_i, number of repetitions r_i, RU type q_i, and the resource assignment u_i for each device i. Then, for each feasible RU type q_i, we select the best triplet of MCS, number of repetitions, and resource assignment (m_i, r_i, u_i) maximizing the energy efficiency. In this way, we will end up with a maximum of four different link adaptation combinations for each UE i. Now, as we are selecting for each RU type q_i, a unique triplet of (m'_i, r'_i, u'_i), the energy efficiency in the resource allocation phase can be expressed in terms of the RU type only as $EE_{i,q}$. Also, since the subcarrier indication field value l determines the RU type q, the energy efficiency can be expressed as $EE_{i,l}$.

In the uplink resource allocation, the BS aims to maximize the network energy efficiency by associating the best UEs to the available candidates, while allocated the best feasible pair of subcarrier indication field $I^{sc}_{i,l}$ and the scheduling delay value $k_{0_{i,k}}$. The pair is considered feasible if the allocation constraints and delay requirements are satisfied. We can write the resource allocation optimization problem as follows:

$$\max_{\eta_{i,j}\theta_{i,l,k}} \sum_{i=1}^{I} \sum_{j=1}^{J} \sum_{l=1}^{L} \sum_{k=1}^{K} \eta_{i,j}\theta_{i,l,k} EE_{i,l} \tag{28}$$

satisfying the constraints (18) to (26), where $\theta_{i,l,k}$ is a binary allocation variable defined to indicate if a device i is allocated a subcarrier indication value l and a scheduling delay value k as follows:

$$\theta_{i,l,k} = \begin{cases} 1, & \text{if device } i \text{ is allocated subcarrier indication} \\ & \text{value } l \text{ and scheduling delay value } k \\ 0, & \text{otherwise.} \end{cases} \tag{29}$$

The defined notations are summarized in Table 8.

V. RESOURCE ALLOCATION IN NB-IoT BASED ON FOUR-SIDED MATCHING GAME

Game theory can be used to study the interaction among different types of interdependent selfish and rational players [7]. Matching problems can be modeled as one-to-one matching, many-to-one matching, and many-to-many matching. Radio resource allocation problems can be modelled as many-to-many matching, where the players are the users and the resources. However, many-to-many matching problems support up to two or three distinct players. In this paper, we aim to study the joint resource allocation and the Candidate-UE association problems. Accordingly, we can distinguish four different types of players: the devices, the available candidates, the subcarrier indication field, and the scheduling delay values. This makes the many-to-many matching problem not suitable for the introduced joint problem.

To model the joint optimization problem, we propose a four-sided matching game, where the players are ranked depending on a preference metric to get the optimal matching. Then, we describe the concept of stable matching as a solution for the formulated four-sided matching game [26]. Next, we develop a four-sided stable matching algorithm that searches for the optimal matches for the joint optimization problem.

TABLE 8. Notations.

Symbol	Description
I	Number of devices
$\mathfrak{T}$	Set of devices
i	Integer variable identifying a device
D	Size of the uplink data (in bits)
p_t	Transmission power
p_t^{min}	Minimum transmission power
p_t^{max}	Maximum transmission power
d	Delay deadline (in milliseconds)
R_{max}	System parameter determining the NP length
G	System parameter determining the NP length
N	length of the NP
r_{DCI}	Number of times a DCI is repeated
J	Number of candidates within an NP
$\mathfrak{J}$	Set of candidates in an NP
j	Integer variable indicating a candidate
$\eta_{i,j}$	Binary association variable indicating if a device i is associated to a candidate j
I^{sc}	Subcarrier indication field
I^{rep}	Repetition number field
I^{RU}	Resource assignment field
I^{MCS}	Modulation and coding scheme field
I^{delay}	Scheduling delay field
y	RU type
q	Integer variable identifying the RU type
p	Integer variable identifying an NP
$v_{p,i,q}$	Binary variable indicating if RU type q is allocated to device i in NP p
t	Duration of a RU
β	Number of subcarriers
$\mathfrak{L}$	Set of subcarrier indication field values
l	Integer variable indicating a subcarrier indication field values
n^{sc}	Subcarriers set
r	Repetition number value
u	Resource assignment value
m	Modulation and coding scheme level
$\mathfrak{K}$	Set of scheduling delay values
k	Integer variable indicating a scheduling delay value
k_{0_k}	Scheduling delay value
$n_{p,i}$	Last NPDCCH subframe carrying the last DCI of device i in NP p
$sb_{p,i}$	First NPUSCH subframe for device i in NP p
DR	Data Rate
CE	Consumed Energy
EE	Energy Efficiency
S_{rx}	Received signal-to-noise ratio
S_{req}	Required signal-to-noise ratio
G_t	Transmitter antenna gain
G_r	Receiver antenna gain
L_{shadow}	Shadow fading effect
L_{path}	Path loss
$L_{penetration}$	Penetration loss
w	Bandwidth of the RU
N_0	Receiver noise spectral density
f	Interference level
$\gamma = 1$	Indoor device
$\gamma = 0$	Outdoor device
σ	Channel estimation error
R_b	Transmission bit rate (bits/s)
B_{eff}	Bandwidth efficiency of NB-IoT technology
S_{eff}	SNR efficiency of NB-IoT technology
c_1 and c_2	Constants obtained using the link-level simulations
C	CRC
B	Transport block size (bits)
B_{max}	Maximum TBS
$x_{p,s,c,i}$	Binary allocation variable indicating if subcarrier c at subframe s in NP p is allocated to device

TABLE 8. *(Continued.)* Notations.

$\theta_{i,l,k}$	Binary allocation variable indicating if a device i is allocated a subcarrier indication value l and a scheduling delay value k
$\phi = (i, j, k, l)$	Many-to-many matching quadruple
Φ	Four-sided many-to-many matching game
$\prec_j$	Preference list of each candidate j over other partners
$\prec_{\mathfrak{J}} = \{\prec_j\}_{j \in J}$	Preference set of candidates
ϕ_j^A	Add matching for candidate j
ϕ_j^S	Swap matching for candidate j
Φ_j^B	Blocking matching for candidate j
$\mathcal{T}_i$	Preference list, containing all the possible pairs of k and l, constructed based on energy efficiency
Γ_j	Rejection list of candidate j

A. MODELLING THE JOINT PROBLEM USING FOUR-SIDED MATCHING GAME

The joint optimization problem aims to maximize the network energy efficiency, through associating the available candidates to the best devices while allocated the appropriate subcarrier indication field and the scheduling delay values. In this subsection, the joint optimization problem of resource allocation and the Candidate-UE association is formulated as a four-sided matching game. The candidates rank the UEs, subcarrier indication fields, and the scheduling delay values based on their corresponding preference list through computing the EE as in (9). The association of UE i to candidate j while allocated scheduling delay k with subcarrier indication l is referred to many-to-many matching quadruple as in:

$$\phi = (i, j, k, l), \quad \forall i \in \mathfrak{T}, j \in \mathfrak{J}, k \in \mathfrak{k}, l \in \mathfrak{L}. \tag{30}$$

Equation (31) expresses the mutual relationship of the matching quadruple as follows:

$$\phi(j, k, l) = (i) \Leftrightarrow \phi(i, k, l) = (j) \Leftrightarrow \phi(i, j, l) = (k) \Leftrightarrow \phi(i, j, k) = (l) \tag{31}$$

Now, we can define the four-sided many-to-many matching game $\Phi = \{\phi, \mathfrak{T}, \mathfrak{J}, \mathfrak{k}, \mathfrak{L}\}$ as a function from the set $\mathfrak{T} \cup \mathfrak{J} \cup \mathfrak{k} \cup \mathfrak{L}$ mapped into the set $\mathfrak{T} \cup \mathfrak{J} \cup \mathfrak{k} \cup \mathfrak{L}$, satisfying the delay requirements and the resource allocation constraints, in addition to the conditions (32) and (33) corresponding to the association constraints in (25) and (26) respectively.

$$|\, \phi(i) \,| \leq 1, \quad \forall i \in \mathfrak{T} \tag{32}$$

$$|\, \phi(j) \,| \leq 1, \quad \forall j \in \mathfrak{J} \tag{33}$$

B. PREFERENCE

The players in the matching game Φ are described as rational and selfish. The optimal matching is decided based on preference. The objective of the joint problem is to maximize the network's energy efficiency. Accordingly, we define the preference as maximizing energy efficiency. From a candidate's perspective, each candidate aims to be associated with the best partners maximizing energy efficiency. Therefore, we build the preference list $\prec_j$ of each candidate over other partners through calculating the corresponding EE using (9). Then, these partners are ranked based on their EE in descending order. Accordingly, in the four-sided matching game, each of i, j, k, and l have preferences over $\mathfrak{J} \times \mathfrak{k} \times \mathfrak{L}$, $\mathfrak{I} \times \mathfrak{k} \times \mathfrak{L}$, $\mathfrak{I} \times \mathfrak{J} \times \mathfrak{L}$, and $\mathfrak{I} \times \mathfrak{J} \times \mathfrak{k}$, respectively, as described below:

- $(j, k, l) \prec_i (j', k', l') \iff EE_{i,l} < EE_{i,l'}$
- $(i, k, l) \prec_j (i', k', l') \iff EE_{i,l} < EE_{i',l'}$
- $(i, j, l) \prec_k (i', j', l') \iff EE_{i,l} < EE_{i',l'}$
- $(i, j, k) \prec_l (i', j', k') \iff EE_{i,l} < EE_{i',l}$

We represent the preference set of devices, candidates, I^{sc}s, and k_0s as $\prec_{\mathfrak{I}}= \{\prec_i\}_{i\in I}$, $\prec_{\mathfrak{J}}= \{\prec_j\}_{j\in J}$, $\prec_{\mathfrak{L}}= \{\prec_l\}_{l\in L}$, $\prec_{\mathfrak{k}}= \{\prec_k\}_{k\in K}$, respectively. Fig. 2 presents an illustrative example of four-sided matching, where three matching quadruples are formed from the available UEs, candidates, I^{sc}s, and k_0s.

C. STABLE MATCHING

Each player aims to maximize its EE through matching with the best partners. However, the energy efficiency of a candidate also depends on the existing matchings. Stable matching solves this interdependency among the players, which is also known as externalities [7]. Stable matching is achieved through enabling candidates to switch their current associated partners. The process of switching is achieved through add matching or swap matching defined as follows:

1) ADD MATCHING

A candidate can switch the current partners by adding a new matching, defined as add matching. Equation (34) expresses the add matching for candidate j denoted by ϕ_j^A.

$$\phi_j^A = \{(i, j, k, l) \cup (i', j, k', l')\} \tag{34}$$

2) SWAP MATCHING

A candidate can switch the current partners by swapping another matching, defined as swap matching. Equation (35) expresses the swap matching for candidate j denoted by ϕ_j^S.

$$\phi_j^S = \{\Phi \backslash \{(j, s, D(s)), (j', s', D(s'))\}\} \cup \{(j, s', D(s')), (j', s, D(s))\} \tag{35}$$

s denotes an arbitrary combination of elements in $\{j, k, l\}$, and $D(s)$ is the set $\{j, k, l\}$ excluding s.

Fig. 3 shows an illustrative example of add and swap matching.

a: BLOCKING MATCHING

We can introduce the concept of blocking matching. Blocking matching is an add or swap matching giving energy efficiency higher than the current selected matching for a player, while satisfying the constraints. Accordingly, in a four-sided matching game, a blocking matching Φ_j^B for candidate j is a matching ϕ_j satisfying conditions 1 and 3, or conditions 2 and 3 as follows:

1) $\exists \quad i' \in \mathfrak{I}, k' \in \mathfrak{k}, l' \in \mathfrak{L}, EE(\phi_j^A) \gtrsim EE(\phi_j)$;
2) $\exists \quad s \in \mathfrak{I} \cup \mathfrak{k} \cup \mathfrak{L}, EE(\phi_j^S) \gtrsim EE(\phi_j)$;
3) The constraints (18) to (26) are satisfied for candidate j in ϕ_j^A or ϕ_j^S.

Utilizing the concept of blocking matching, the current matching ϕ_j for candidate j is considered stable, if there is no more blocking matching ϕ_j^B.

Algorithm 1 Four-Sided Many-to-Many Matching Algorithm

Phase I - Initialization:
Data: $\mathfrak{I}, \mathfrak{J}, \mathfrak{k}, \mathfrak{L}$.
Output: The matching set Φ
The preference list of unit $\mathcal{T}$ is constructed for each device i, $i \in \mathfrak{I}$, where $t_i(k, l) \in \mathcal{T}_i$, by calculating $EE_{i,l}$ using (9).
Each candidate j, $j \in \mathfrak{J}$, is associated to the best free device i, $i \in \mathfrak{I}$, giving the highest EE. The associated pair a is stored in set A, such that $a = (i, j) \in \mathcal{A}$.
forall $j \in \mathfrak{J}$ **do**
  check its associated device i, where $i = a(j)$
  $O = 0$
  while $O == 0$ **do**
    forall $t_i \in \mathcal{T}$ **do**
      if (18)**to**(24) **then**
        Output the matching:
        $\phi_j = (UE_i, CN_j, I_l^{sc}, k_{0_k}), \phi_j \in \Phi$
        $O = 1$;
        break;
      $t = t + 1$;
    if $O == 0$ **then**
      Discard the UE i;
      Search for another free UE i', not associated to another candidate j', with high EE.
      $i = i'$

Phase II - Updating existing matching:
Input: the matching set Φ and the reject list Γ
forall $j \in \mathcal{J}$ **do**
  forall $\phi_j \in \Phi$ **do**
    while $\exists \phi_j^B$ *and* $\phi_j^B \notin \Gamma_i$ **do**
      $\phi_j' = \phi_j^B$
      if *(25) & (26)* **then**
        candidate j holds the current matching ϕ_j';
      else
        Discard candidate j' associated to UE i;
        Add $\phi_{j'}$ into $\Gamma_{j'}$;
        candidate j' re-match to the next best free UE.
      Add ϕ_j into Γ_j,

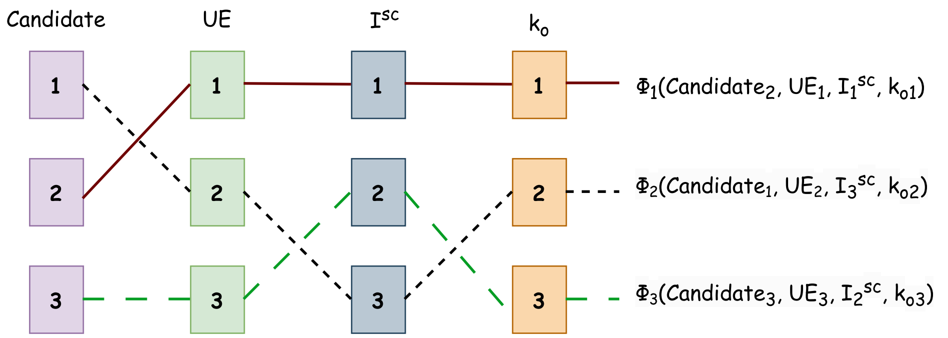

FIGURE 2. An illustrative example of four-sided many-to-many matching, where three matching quadruples are formed.

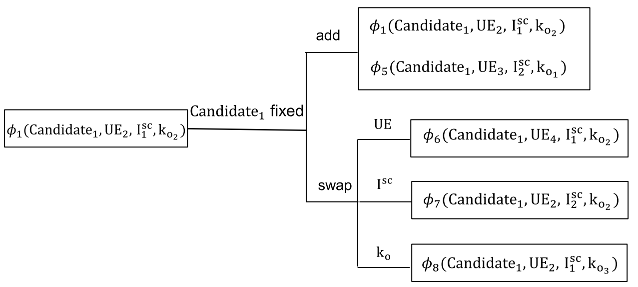

FIGURE 3. An illustrative example of add and swap matching. For a fixed candidate$_1$, we can add ϕ_5 to its existing matching ϕ_1. Also, ϕ_6, ϕ_7, and ϕ_8 are examples of swap matching for ϕ_1, obtained by swapping its current partner UE, I^{sc}, and k_o respectively.

D. FOUR-SIDED MANY-TO-MANY MATCHING ALGORITHM

In this part, we develop a four-sided many-to-many matching algorithm (FSMTMA) to achieve stable matching. Algorithm 1 describes the steps applied in the developed algorithm (FSMTMA). FSMTMA is divided into two phases: Initialization, and Updating existing matching.

In the Initialization phase, each candidate j is associated to the best available UE i with the profitable pair of subcarrier indication field value l, and scheduling delay value k. First, we define, for each UE i, a preference list of unit $\mathcal{T}_i$, $t_i(k, l) \in \mathcal{T}_i$, containing all the possible pairs of scheduling delay value (k) and subcarrier indication value (l). The preference list is constructed based on energy efficiency (EE). Then, in step 2, each candidate j associates to the most profitable UE i, not associated to another candidate. The associated pair is denoted by a and stored in set $\mathcal{A}$. In steps 4 to 18, we select for each pair $a \in \mathcal{A}$, the best pair t_i of scheduling delay value k and subcarrier indication field l satisfying the delay and allocation constraints. In case no feasible pair $t_i = (k, l)$ for the association a, the candidate j discards the current UE i and rematches with other profitable free UE.

After the Initialization phase, phase II aims to achieve stability through checking whether there is a blocking matching for each candidate j as shown in steps 19 to 30. Starting with the first candidate j, if there is blocking matching ϕ_j^B, check if the association constraints (25) and (26) are satisfied. If constraints are satisfied, candidate j chooses the blocking matching ϕ_j^B and adds ϕ_j to its rejection list Γ_j. If association constraints are not satisfied, discard candidate j' associated to UE i of the blocking matching. Add the current matching $\phi_{j'}$ of j' into its rejection list $\Gamma_{j'}$. Then, j' rematches to the next best free UE. The same process is repeated until no more blocking matching exists for DCI j.

VI. PERFORMANCE EVALUATION

In this section, we aim to compare the performance of the proposed four-sided many-to-many matching algorithm (FSMTMA) to three heuristic methods: maximum signal-to-noise ratio (Max-SNR), maximum spectral efficiency (Max-SE), and random selection (RD). Each Max-SNR and Max-SE sorts the devices based on their SNR and spectral efficiency respectively, while the random selection method selects randomly the devices to be served. These sorted devices are stored in a set. Then, starting from the first device in the set, the optimal combination of the parameters maximizing the energy efficiency is obtained.

We consider 200 devices uniformly distributed in a circular area. Devices are placed at a distance ranging from 7 km to 10 km from the BS. We assume that the size of the packet transmitted by each device is 50 bytes. Each device has a delay requirement value ranging from 1000 ms to 6000 ms. We obtained the results using MATLAB. Table 9 shows the simulation parameters.

We consider 50 different realizations with different radio conditions to obtain statistically significant analysis with 95% confidence interval. Okumura-Hata propagation model is utilized to compute path loss.

Fig. 4 describes the variation in the average number of served devices in the different methods: FSMTMA, Max-SE, Max-SNR, and RD. In this paper, we consider the number of candidates is equal to 8. Accordingly, the maximum number of served devices per NP cannot exceed 8. We can observe that all the methods can serve the maximum number of devices in each realization. However, the average number of served devices in the Max-SNR method (7.76) is slightly smaller. This is because the Max-SNR method serves devices with good channel qualities regardless of the number of packets that these devices need to transmit. In other words,

TABLE 9. The simulation parameters.

Parameter	Value
Maximum Transmit Power (p_t^{max})	23 dBm
Minimum Transmit Power (p_t^{min})	-40 dBm
Antenna Gain of Receiver (G_r)	9 dBi
Antenna Gain of Transmitter (G_t)	0 dBi
Thermal Noise Density (N_0)	-174 dBm/Hz
Request Data Size (D)	50 bytes
Delay Value (d)	1000 to 6000 ms
Interference Margin	3 dBm
Number of NPDCCH Subframes (R_{max})	256
Length of NPDCCH Period (N)	4096
Number of candidates in NP (J)	8

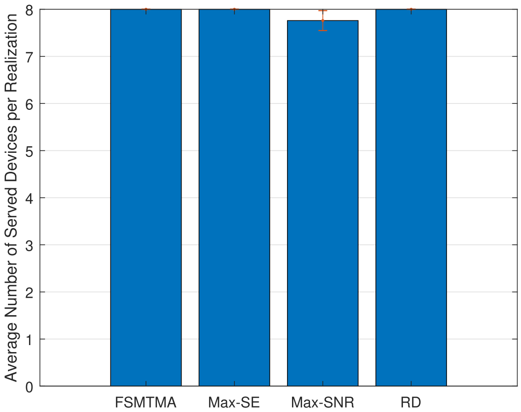

FIGURE 4. Variation in the average number of served devices per realization.

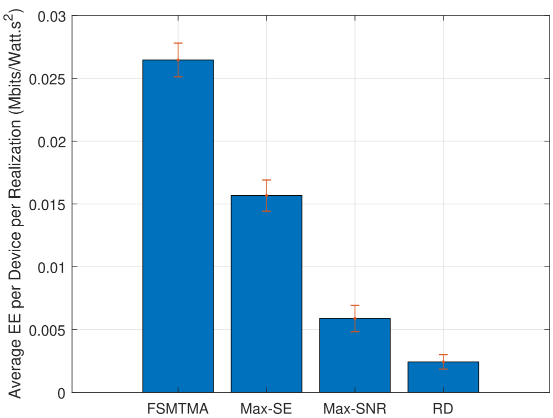

FIGURE 5. Variation in the average energy efficiency per device per realization.

the selected devices with good radio conditions could need to send many packets, ending up occupying too many resources, and thus decreasing the left resources for remaining devices.

Fig. 5 shows the variation in the obtained average energy efficiency per device in each of FSMTMA, Max-SE, Max-SNR, and RD, respectively. We can observe that the FSMTMA can achieve the highest average EE (0.025 Mbits/Watt.s^2) as the EE is the preference when selecting the best quadruple for each candidate. Also, we can notice that the Max-SE method achieves higher average

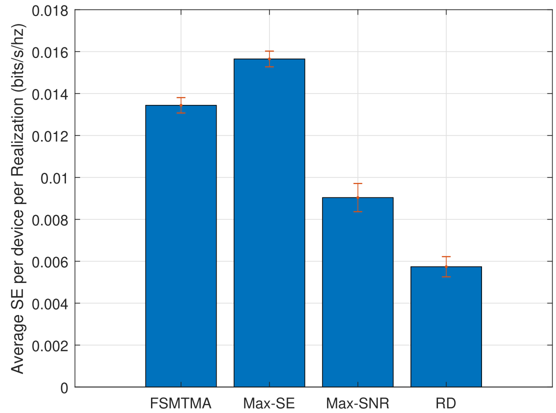

FIGURE 6. Variation in the average spectral efficiency per device per realization.

EE (0.01567 Mbits/Watt.s^2), compared to the Max-SNR, (0.005882 Mbits/Watt.s^2), and RD (0.002431 Mbits/Watt.s^2), methods. This is because the Max-SE method gives higher priority for devices with better spectral efficiency. Such devices try to transmit their data with short transmission duration ending up with higher energy efficiencies.

Fig. 6 presents the variation in the obtained average spectral efficiency per device in each of FSMTMA, Max-SE, Max-SNR, and RD, respectively. We can observe that the Max-SE method achieves the highest spectral efficiency (0.01565 bits/s/Hz), as it gives higher priority for devices with higher spectral efficiency. The FSMTMA method achieves average spectral efficiency (0.01344 bits/s/Hz) greater than that achieved in the Max-SNR (0.009037 bits/s/Hz) and the RD (0.00574 bits/s/Hz) methods. FSMTMA method aims to maximize network energy efficiency. Accordingly, the selected devices transmit their data with short transmission duration ending up with improved spectral efficiency. Max-SNR method selects devices with good radio conditions regardless of the number of packets to be transmitted. Such devices could need longer transmission duration, implies more allocated subframes, ending up with reduced spectral efficiency.

To study the significance of the variations presented in Figs. 5 and 6, we study the variation of the ratio of the energy efficiency over the spectral efficiency per device per realization as shown in Fig. 7. The spectral efficiency is defined as the data rate over the bandwidth of the allocated RU type. Accordingly, the ratio can be expressed as:

$$ratio = \frac{\beta}{u \cdot t \cdot r}, \tag{36}$$

where $u \cdot t \cdot r$ denotes the transmission duration. We can observe that the FSMTMA method achieves the highest value of the ratio compared to the Max-SE, Max-SNR, and RD methods where each of FSMTMA, Max-SE, Max-SNR, and RD method achieves an average value equal to 1.15 Hz/s, 0.9316 Hz/s, 0.4498 Hz/s, and 0.2508 Hz/s, respectively. As the FSMTMA method considers energy efficiency as a

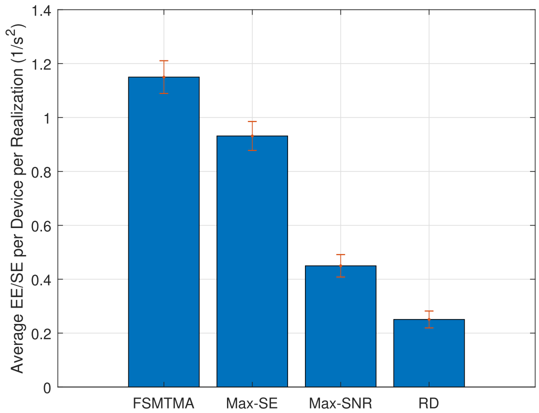

FIGURE 7. Variation in the average ratio of energy efficiency over spectral efficiency per device per realization.

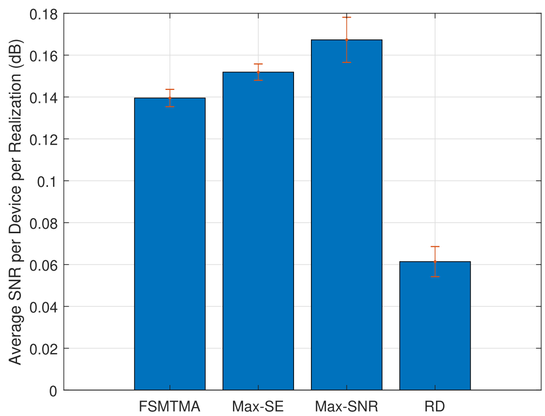

FIGURE 8. Variation in the average SNR per device per realization.

preference, the selected devices transmit their packets with a lower transmission duration, ending up with improved value of the ratio. The selected devices in the Max-SE method improve the overall spectral efficiency. Improving the spectral efficiency can be achieved through decreasing the transmission duration to reduce the number of allocated resources per device. This ends up with an improved average of the ratio. Max-SNR and RD methods achieve the lowest average ratio, as they do not consider the allocated resources when selecting the devices to be served.

Fig. 8 describes the variation in the obtained average SNR per device per realization. We can observe that the highest average (0.1673 dB) is achieved in the Max-SNR method as it gives higher priority for devices with better SNR. Max-SE and FSMTMA methods achieve lower average SNR per device per realization where an average of 0.1519 dB and 0.1395 dB are achieved in the Max-SE and FSMTMA methods, respectively. This is because both Max-SE and FSMTMA methods prefer devices with smaller transmission durations regardless of their received SNR values. However, Max-SNR, Max-SE, and FSMTMA methods prefer devices transmitting their data on narrower band to boost the SNR, improve the spectral efficiency, and enhance the energy

TABLE 10. Average computational time per realization (s).

Method	FSMTMA	Max-SE	Max-SNR	RD
computational time (s)	65.657	63.19	63.215	63.22

efficiency, respectively. This explains the stark difference in the averages achieved in these three methods and the average achieved in the RD method (0.06138 dB).

VII. DISCUSSION

Based on the analysis of Figs. 4 to 8, we can infer that FSMTMA method outperforms the Max-SE, Max-SNR, and RD methods in terms of energy efficiencies and the ratio of the energy efficiency over the spectral efficiency per device, but with slightly higher computational efficiency and lower average SNR. Table 10 shows that the FSMTMA method achieves slightly greater computational efficiency compared to Max-SE, Max-SNR, and RD methods where the average computational time achieved in the FSMTMA, Max-SE, Max-SNR, and RD methods is equal to 65.657s, 63.19s, 63.215s, and 63.22s respectively represented in Table 10. This slight increase in the average computational time is due to phase II in the FSMTMA method. FSMTMA gives higher priority for devices with better energy efficiency, as the preference is the energy efficiency in the proposed algorithm. Devices with better energy efficiencies can transmit their packets with shorter transmission durations. This boosts the spectral efficiency regardless of the resulting received SNR.

Based on the analysis done in our previous work [5], we revealed the impact of the RU type parameter in improving the spectral efficiency, and achieving efficient resource allocation. That is because the RU type specifies the number of subframes, and subcarriers occupied by one RU. For this reason, we formulate our joint optimization problem considering this parameter represented by the subcarrier indication field. Also, selecting the combination of the remaining parameters (number of repetitions, resource assignments, and MCS level) while maximizing the energy efficiency, for each RU type in the link adaptation, serves in improving the spectral efficiency. The selected number of repetitions and the resource assignments, in addition to the duration of the RU type determine the transmission duration, thus the total number of the uplink subframes allocated to a device. Accordingly, maximizing the energy efficiency ends up with reduced number of the allocated subframes, as maximizing the energy efficiency is proportional to minimizing the transmission duration.

VIII. CONCLUSION

In this paper, we investigated the joint optimization of resource allocation procedure and Candidate-UE association in NB-IoT networks on the uplink. Our objective is to maximize the network's energy efficiency while satisfying reliability, delay, and resource allocation constraints. To model the many-to-many matching among the candidates, UEs, subcarrier indication fields, and the scheduling delay, we resorted to a four-sided matching game. We proposed a four-sided stable matching algorithm to get the best matchings. Simulation results highlighted the performance of the proposed algorithm by comparing it with other algorithms.

In this paper, we investigated the joint optimization of resource allocation procedure and Candidate-UE association in NB-IoT networks on the uplink. Our objective is to maximize the network's energy efficiency while satisfying reliability, delay, and resource allocation constraints. To model the many-to-many matching among the candidates, UEs, subcarrier indication fields, and the scheduling delay, we resorted to a four-sided matching game. We proposed a four-sided stable matching algorithm to get the best matchings. Simulation results highlighted the performance of the proposed algorithm by comparing it with other standard algorithms in terms of the average energy efficiency achieving 37.32% to 90.27% improvements. For future work, we will investigate the scheduling problem in NB-IoT considering multi-cellular networks, and the resulting intercell interference (ICI).

REFERENCES

[1] Y.-P.-E. Wang, X. Lin, A. Adhikary, A. Grovlen, Y. Sui, Y. Blankenship, J. Bergman, and H. S. Razaghi, "A primer on 3GPP narrowband Internet of Things," *IEEE Commun. Mag.*, vol. 55, no. 3, pp. 117–123, Mar. 2017.

[2] *Cellular System Support for Ultra-Low Complexity and Low Throughput Internet of Things (CIoT) (Rel-13)*, Standard 3GPP TR 45.820 V13.1.0, Tech. Rep., 2015.

[3] *Ericsson Mobility Report*, Ericsson, Stockholm, Sweden, 2022.

[4] L. Feltrin, G. Tsoukaneri, M. Condoluci, C. Buratti, T. Mahmoodi, M. Dohler, and R. Verdone, "Narrowband IoT: A survey on downlink and uplink perspectives," *IEEE Wireless Commun.*, vol. 26, no. 1, pp. 78–86, Feb. 2019.

[5] F. Yassine, M. El Helou, S. Lahoud, and O. Bazzi, "Energy-efficient uplink scheduling in narrowband IoT," *Sensors*, vol. 22, no. 20, p. 7744, Oct. 2022.

[6] *Evolved Universal Terrestrial Radio Access (E-UTRA);Physical Layer Procedures*, Standard 3GPP TS 36.213 V14.3.0, Technical Specification Group Radio Access Network, 2017.

[7] S. Bayat, Y. Li, L. Song, and Z. Han, "Matching theory: Applications in wireless communications," *IEEE Signal Process. Mag.*, vol. 33, no. 6, pp. 103–122, Nov. 2016.

[8] A. Hazra, P. K. Donta, T. Amgoth, and S. Dustdar, "Cooperative transmission scheduling and computation offloading with collaboration of fog and cloud for industrial IoT applications," *IEEE Internet Things J.*, vol. 10, no. 5, pp. 3944–3953, Mar. 2023.

[9] J. Liu, C.-H.-R. Lin, Y.-C. Hu, and P. K. Donta, "Joint beamforming, power allocation, and splitting control for SWIPT-enabled IoT networks with deep reinforcement learning and game theory," *Sensors*, vol. 22, no. 6, p. 2328, Mar. 2022.

[10] T.-Y. Wu, R.-H. Hwang, A. Vyas, C.-Y. Lin, and C.-R. Huang, "Persistent periodic uplink scheduling algorithm for massive NB-IoT devices," *Sensors*, vol. 22, no. 8, p. 2875, Apr. 2022.

[11] Y.-J. Yu and L.-X. Li, "Offset-aware resource allocation in NB-IoT networks," *IEEE Internet Things J.*, vol. 9, no. 23, pp. 23967–23980, Dec. 2022.

[12] Q.-S. Hu, X.-N. Fan, and Z.-Y. Li, "A simple and efficient link adaptation method for narrowband Internet of Things," in *Proc. IEEE 21st Int. Conf. High Perform. Comput. Commun.; IEEE 17th Int. Conf. Smart City; IEEE 5th Int. Conf. Data Sci. Syst. (HPCC/SmartCity/DSS)*, Aug. 2019, pp. 2606–2609.

[13] C. Yu, L. Yu, Y. Wu, Y. He, and Q. Lu, "Uplink scheduling and link adaptation for narrowband Internet of Things systems," *IEEE Access*, vol. 5, pp. 1724–1734, 2017.

[14] E. Lujan, J. A. Zuloaga Mellino, A. D. Otero, L. R. Vega, C. G. Galarza, and E. E. Mocskos, "Extreme coverage in 5G narrowband IoT: A LUT-based strategy to optimize shared channels," *IEEE Internet Things J.*, vol. 7, no. 3, pp. 2129–2136, Mar. 2020.

[15] Q. Mu, L. Liu, H. Jiang, K. Takeda, and R. Ma, "Investigation on link adaptation for LTE-based machine type communication," in *Proc. IEEE 83rd Veh. Technol. Conf. (VTC Spring)*, May 2016, pp. 1–5.

[16] P. Andres-Maldonado, P. Ameigeiras, J. Prados-Garzon, J. J. Ramos-Munoz, J. Navarro-Ortiz, and J. M. Lopez-Soler, "Analytic analysis of narrowband IoT coverage enhancement approaches," in *Proc. Global Internet Things Summit (GIoTS)*, Jun. 2018, pp. 1–6.

[17] S. Ravi, P. Zand, M. El Soussi, and M. Nabi, "Evaluation, modeling and optimization of coverage enhancement methods of NB-IoT," in *Proc. IEEE 30th Annu. Int. Symp. Pers., Indoor Mobile Radio Commun. (PIMRC)*, Sep. 2019, pp. 1–7.

[18] F. Yassine, M. E. Helou, O. Bazzi, and S. Lahoud, "Investigation on narrowband IoT link adaptation with rate and energy objectives," in *Proc. Int. Wireless Commun. Mobile Comput. (IWCMC)*, Jun. 2021, pp. 412–417.

[19] F. Yassine, M. El Helou, S. Lahoud, and O. Bazzi, "Performance of narrowband IoT link adaptation with rate and energy objectives," in *Proc. IEEE 3rd Int. Multidisciplinary Conf. Eng. Technol. (IMCET)*, Dec. 2021, pp. 6–10.

[20] H. Malik, H. Pervaiz, M. M. Alam, Y. Le Moullec, A. Kuusik, and M. Ali Imran, "Radio resource management scheme in NB-IoT systems," *IEEE Access*, vol. 6, pp. 15051–15064, 2018.

[21] Y.-J. Yu and J.-K. Wang, "Uplink resource allocation for narrowband Internet of Things (NB-IoT) cellular networks," in *Proc. Asia–Pacific Signal Inf. Process. Assoc. Annu. Summit Conf. (APSIPA ASC)*, Nov. 2018, pp. 466–471.

[22] P.-Y. Liu, K.-R. Wu, J.-M. Liang, J.-J. Chen, and Y.-C. Tseng, "Energy-efficient uplink scheduling for ultra-reliable communications in NB-IoT networks," in *Proc. IEEE 29th Annu. Int. Symp. Pers., Indoor Mobile Radio Commun. (PIMRC)*, Sep. 2018, pp. 1–5.

[23] O. Elgarhy, L. Reggiani, H. Malik, M. M. Alam, and M. A. Imran, "Rate-latency optimization for NB-IoT with adaptive resource unit configuration in uplink transmission," *IEEE Syst. J.*, vol. 15, no. 1, pp. 265–276, Mar. 2021.

[24] Y. Gu, W. Saad, M. Bennis, M. Debbah, and Z. Han, "Matching theory for future wireless networks: Fundamentals and applications," *IEEE Commun. Mag.*, vol. 53, no. 5, pp. 52–59, May 2015.

[25] B. Di, S. Bayat, L. Song, Y. Li, and Z. Han, "Joint user pairing, subchannel, and power allocation in full-duplex multi-user OFDMA networks," *IEEE Trans. Wireless Commun.*, vol. 15, no. 12, pp. 8260–8272, Dec. 2016.

[26] C. Dai, K. Zhu, Z. Li, and E. Hossain, "Joint decoupled multiple-association and resource allocation in full-duplex heterogeneous cellular networks: A four-sided matching game," *IEEE Trans. Wireless Commun.*, vol. 21, no. 8, pp. 6464–6477, Aug. 2022.

[27] S. Metwaly, A. A. El-Haleem, and O. El-Ghandour, "NOMA based matching game algorithm for narrowband Internet of Things (NB-IoT) system," *Ingénierie des Systèmes d Inf.*, vol. 25, no. 3, pp. 345–350, Jun. 2020.

[28] *Evolved Universal Terrestrial Radio Access(EUTRA); Radio Resource Control (RRC); Protocol Specification*, Standard 3GPP TS 36.331 V14.2.2, Technical Specification Group Radio Access Network, 2017.

[29] Y.-J. Yu, "NPDCCH period adaptation and downlink scheduling for NB-IoT networks," *IEEE Internet Things J.*, vol. 8, no. 2, pp. 962–975, Jan. 2021.

[30] P. Andres-Maldonado, P. Ameigeiras, J. Prados-Garzon, J. Navarro-Ortiz, and J. M. Lopez-Soler, "An analytical performance evaluation framework for NB-IoT," *IEEE Internet Things J.*, vol. 6, no. 4, pp. 7232–7240, Aug. 2019.

[31] *Consideration on Uplink Data Transmission for NB-IoT*, Standard r1-160480, 3GPP, 2016.

[32] *Further Consideration on NB-PDSCH Design for NB-IoT*, Standard r1-1703113, 3GPP, Sophia Antipolis, France, 2017.

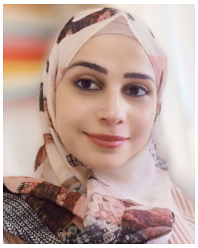

FARAH YASSINE received the bachelor's degree in computer and communication engineering from the Islamic University of Lebanon, in 2018, and the master's degree from Lebanese University, in 2019. She is currently pursuing the dual Ph.D. degree with the Faculty of Engineering, Ecole Supérieure d'Ingénieurs de Beyrouth (ESIB), Saint Joseph University of Beirut, and Lebanese University. Her thesis focuses on resource allocation and optimization in narrowband IoT.

MELHEM EL HELOU (Senior Member, IEEE) received the engineering and master's degrees in telecommunications and networking engineering from Ecole Supérieure d'Ingénieurs de Beyrouth (ESIB), Saint Joseph University of Beirut, Beirut, Lebanon, in 2009 and 2010, respectively, and the Ph.D. degree in computer and telecommunications engineering from IRISA Research Institute, University of Rennes, France, and Saint Joseph University of Beirut, in 2014. He joined ESIB, in September 2013, where he is currently an Associate Professor. His teaching and research interests include wireless networking, cellular technologies, Internet of Things, network virtualization, and quality of service.

SAMER LAHOUD received the Ph.D. degree in computer science and networks from IMT Atlantique, Rennes, and the Habilitation degree from the University of Paris-Saclay, in 2023, for his work on optimizing radio resource allocation in cellular networks. He has been with the University of Rennes, since 2007. He was a Visiting Scholar with Saint Joseph University, Beirut, Lebanon, from 2016 to 2022. In addition, he was a Research Engineer with the Nokia Bell Laboratories Europe, from 2016 to 2017. He is currently an Associate Professor with the University of Rennes and a Researcher with the IRISA Laboratory, France. His research interest includes radio resource allocation problems in wireless communication networks.

OUSSAMA BAZZI received the B.E. degree in electrical engineering from the American University of Beirut (AUB), in 1987, and the master's and Ph.D. degrees in electronics from the University of Valenciennes and Hainaut Cambresis (UVHC), France, in 1988 and 1992, respectively. He joined Lebanese University, in 1996, where he is currently a Full Professor and the Head of the Master Program Signals, Telecoms, Image, and Speech (STIP). His research interests include signal processing, spectrum sensing, wireless, and mobile radio communications. His current research interests include resource allocation and optimization, hybrid broadcast systems, cooperative communication techniques, and cognitive radio networks.